The E3 ubiquitin ligase Pib1 regulates effective gluconeogenic shutdown upon glucose availability

Received for publication, June 18, 2019, and in revised form, September 27, 2019 Published, Papers in Press, October 11, 2019, DOI 10.1074/jbc.RA119.009822

Vineeth Vengayil[‡§], **Zeenat Rashida**[‡§], **and Sunil Laxman**[‡1]

From the [‡]*Institute for Stem Cell Science and Regenerative Medicine (inStem), GKVK Post, Bellary Road, Bangalore 560065, India and the* [§]*Manipal Academy of Higher Education, Manipal, Karnataka 576104, India*

Edited by George N. DeMartino

Cells use multiple mechanisms to regulate their metabolic states in response to changes in their nutrient environment. One example is the response of cells to glucose. In *Saccharomyces cerevisiae* growing in glucose-depleted medium, the re-availability of glucose leads to the down-regulation of gluconeogenesis and the activation of glycolysis, leading to "glucose repression." However, our knowledge of the mechanisms mediating the glucose-dependent down-regulation of the gluconeogenic transcription factors is limited. Using the major gluconeogenic transcription factor Rds2 as a candidate, we identify here a novel role for the E3 ubiquitin ligase Pib1 in regulating the stability and degradation of Rds2. Glucose addition to cells growing under glucose limitation results in a rapid ubiquitination of Rds2, followed by its proteasomal degradation. Through *in vivo* and *in vitro* experiments, we establish Pib1 as the ubiquitin E3 ligase that regulates Rds2 ubiquitination and stability. Notably, this Pib1-mediated Rds2 ubiquitination, followed by proteasomal degradation, is specific to the presence of glucose. This Pib1-mediated ubiquitination of Rds2 depends on the phosphorylation state of Rds2, suggesting a cross-talk between ubiquitination and phosphorylation to achieve a metabolic state change. Using stable isotope-based metabolic flux experiments, we find that the loss of Pib1 results in an imbalanced gluconeogenic state, regardless of glucose availability. Pib1 is required for complete glucose repression and enables cells to optimally grow in competitive environments when glucose again becomes available. Our results reveal the existence of a Pib1-mediated regulatory program that mediates glucose repression when glucose availability is restored.

The uptake and utilization of nutrients are essential for cell growth and survival. Multiple metabolic pathways within cells make and break nutrients, and these pathways are tightly regulated depending on nutrient availability (1, 2). Because the nutrient environment of a cell is not constant, particularly for free-living microbes, cells rewire their metabolic pathways depending on the changes in nutrient availability (3–5). This ability of cells to rapidly and efficiently switch between different metabolic states is crucial for their survival and is closely coupled to the nutrient-sensing machinery (6–8). Therefore, cells integrate multiple strategies to carry out efficient metabolic switching. Understanding these strategies are major areas of study.

Saccharomyces cerevisiae is an excellent model to decipher conserved general principles of metabolic state switching, due to the ease of controlling its metabolism (by altering nutrients provided) coupled with genetic and biochemical approaches to dissect regulatory mechanisms. A feature of *S. cerevisiae* metabolism is a strong preference for glucose as a carbon source, where cells preferentially ferment glucose (9). This is the famous "Crabtree effect," analogous to the Warburg effect in cancer cells, where cells use glucose over other available carbon sources and minimize respiratory metabolism when glucose is present (9–11). Therefore, glucose availability regulates a variety of cellular responses in yeast (12–14). Following glucose limitation, cells switch to a gluconeogenic state where alternative carbon sources are utilized, and upon glucose re-entry, cells switch back to a glycolytic state where alternative carbon source utilization is repressed (15). Therefore, efficient glucose-induced catabolite repression is critical to ensure that upon glucose re-entry gluconeogenesis is shut down (16–18). The initial responses involved in glucose repression occur immediately after glucose addition, through rapid changes in intracellular metabolite pools driven by allosteric regulations and metabolic flux rewiring (19–21). Subsequently, proteins that enforce the metabolic state switch are regulated by the interplay of different transcriptional, translational, post-transcriptional, and post-translational responses (22). Post-translational regulation (by signaling-mediated events) allows rapid and dynamic regulation of protein levels and activity in response to a nutrient such as glucose (23). While we have a growing understanding of signaling and regulatory events controlling cell growth with glucose as a carbon source (24–26), several gaps remain in our understanding of the "off-switches" that enable effective glucose repression in cells.

In particular, we have a limited understanding of how regulated protein turnover controls metabolic state switching when cells encounter a new nutrient source. Our understanding of regulatory events in this condition is biased toward "classic" signaling, through the activation of nutrient-responsive kinases and phosphatases (27–29). Alternative modes of regulation, including selective protein turnover in response to changing

This work was supported by DST-INSPIRE Fellowship DST/INSPIRE/03/2016/001546 (to V. V.) from the Department of Science and Technology, Government of India, Wellcome Trust-DBT India Alliance Intermediate Fellowship IA/I/14/2/501523 (to S. L.), and institutional support from inStem and the Department of Biotechnology, Government of India. The authors declare that they have no conflicts of interest with the contents of this article.

This article contains Figs. S1–S3, Table S1, and supporting File S1.

[1] To whom correspondence should be addressed. E-mail: sunil@instem.res.in.

nutrients (as opposed to "starvation") remain poorly studied. The ubiquitin-mediated proteasomal degradation is a major pathway of selective protein degradation in eukaryotes (30, 31), but the role of the ubiquitin-proteasomal system in regulating metabolic switching is poorly understood. Because target specificity of ubiquitination is achieved by E3 ubiquitin ligases, which bind and specifically target proteins for ubiquitin conjugation (32, 33), there must be distinct E3 ligases activated by unique nutrient cues, which then ubiquitinate their substrates. However, only a few studies identify roles of E3 ubiquitin ligases in the context of glucose-mediated metabolic switching. In yeast, upon glucose depletion, the E3 ligase Grr1 targets the phosphofructokinase (Pfk27) enzyme for degradation, thereby inhibiting glycolysis (34). In the context of catabolite (glucose) repression, the E3 ligase complex SCF_{Ucc1} regulates the degradation of the citrate synthase enzyme Cit2, thereby inhibiting the glyoxylate shunt (35). Furthermore, the GID complex degrades the gluconeogenic enzymes Fbp1 and Pck1 in the presence of glucose (36, 37). Apart from these, little is known about the role of E3 ligases in regulating effective gluconeogenic shutdown. Similar examples from mammalian cells are even rarer (38). Finally, these studies are limited to only the regulation of relevant metabolic enzymes following glucose addition. For a complete metabolic state switch, the transcription factors that regulate these enzyme transcripts must themselves also be regulated. In yeast, Rds2, Cat8, and Sip4 are the transcription factors that regulate gluconeogenic enzyme transcripts during growth in glucose-deplete conditions (1, 39–41). Although these have been well-studied in cells growing under glucose limitation, how these transcription factors are regulated immediately after glucose becomes available has surprisingly not been addressed (Fig. 1*A*).

In this study, we sought to identify novel regulators of glucose repression by focusing on the amount of gluconeogenic transcription factors when glucose becomes available. For this, we used the gluconeogenic transcription factor Rds2 as a candidate protein. Here, we discover that Rds2 is rapidly ubiquitinated and proteasomally degraded upon glucose addition. This is mediated by a specific E3 ubiquitin ligase, Pib1, in a glucose-dependent manner. Through *in vivo* and *in vitro* studies, we show a direct role of Pib1 in mediating glucose-dependent Rds2 ubiquitination and degradation. This Pib1-mediated ubiquitination of Rds2 depends on the phosphorylation state of Rds2. We establish that Pib1 is required for normal gluconeogenic flux in cells and effective gluconeogenic shutdown following glucose re-entry. Collectively, our study identifies a novel role for a previously obscure E3 ubiquitin ligase in regulating gluconeogenic shutdown and thereby facilitating effective glucose repression. More generally, our study exemplifies how E3 ubiquitin ligases can respond to changing nutrients and serve as "on" or "off" switches to regulate cellular metabolic state.

Results

Glucose regulates Rds2 protein levels

The transcription factors Rds2, Cat8, and Sip4 regulate gluconeogenesis under conditions of glucose limitation, by activating the expression of enzymes involved in gluconeogenesis. However, the mechanisms by which these transcription factors are shut down following glucose re-entry are not well-understood (Fig. 1*A*). To understand the processes involved in glucose-mediated regulation of these transcription factors, we chose Rds2 as a candidate, to specifically understand regulation after glucose addition. Using yeast cells with Rds2 chromosomally tagged at the C terminus with a FLAG epitope tag, we monitored the steady-state levels of Rds2 in cells grown in high-glucose medium (2% glucose) or glucose-limited/deplete medium (2% glycerol and ethanol) using Western blottings. The amounts of Rds2 protein was substantially lower in cells in high-glucose medium compared with low-glucose medium (Fig. 1*B*). This suggested the likelihood of an existing mechanism to regulate Rds2 protein levels depending on the availability of glucose. To understand the kinetics of Rds2 protein regulation when cells encounter glucose, we monitored Rds2 protein amounts over time in cells growing in glucose-limited medium (glycerol/ethanol as a carbon source), to which glucose was added to a final concentration of 3%. We observed a rapid decrease in Rds2 amounts after glucose addition (Fig. 1, *C* and *D*), with a significant decrease observed as quickly as ~20 min after glucose addition (Fig. 1*D*). After ~30 min of glucose addition, the amount of Rds2 protein was similar to that of the control (cells grown in 2% glucose medium). No changes in Rds2 amounts were observed when glucose was not added (Fig. 1*C*), reiterating that the change in Rds2 amounts was glucose-dependent. Overall, these results suggest that glucose addition activates a regulatory event that rapidly reduces the amount of Rds2 in cells.

Glucose induces ubiquitination and proteasomal degradation of Rds2

Previous studies have identified roles of the protein degradation machinery in regulating the gluconeogenic enzymes Pck1 and Fbp1 in response to glucose addition (37). Protein degradation plays a role in rapid glucose-mediated catabolite inactivation of many proteins (36, 42). This is expected because decreases in protein amounts can be achieved swiftly via protein degradation, compared with changes in transcription or translation. Considering the decrease in Rds2 amounts within a few minutes after glucose re-entry, we hypothesized that glucose induces degradation of Rds2. Upon inspecting the amino acid sequence of Rds2, we found multiple lysine residues present in the protein (Fig. 2*A*). Because ubiquitination (leading to protein degradation) occurs at the lysine residues of target proteins, we used multiple ubiquitination prediction programs (43–45) to assess whether these lysines were predicted to be ubiquitinated. We found that multiple lysine residues on Rds2 were strongly predicted to be ubiquitination sites (Fig. 2*A* and Fig. S1*A*). To test the possibility that Rds2 might indeed be ubiquitinated and degraded proteasomally, we first investigated whether Rds2 was degraded by the proteasome. We treated cells with the proteasomal inhibitor MG132, and we monitored Rds2 protein amounts post-glucose addition. Notably, Rds2 amounts remained constant after glucose addition (Fig. 2, *B* and *C*), in contrast to cells without MG132 where Rds2 was rapidly degraded. The amounts of Rds2 were significantly higher in cells treated with MG132, compared with untreated

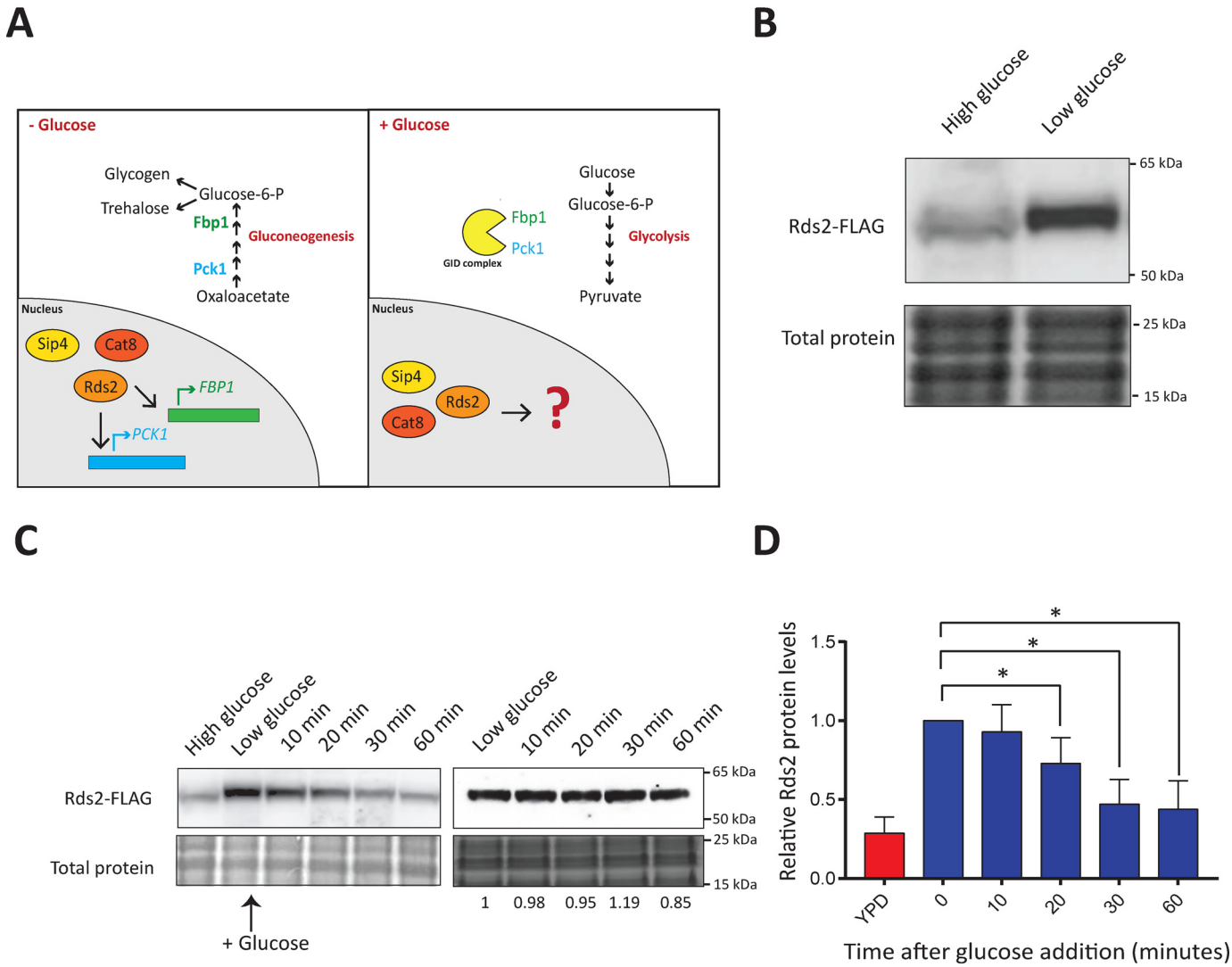

Figure 1. Glucose regulates Rds2 protein levels. *A,* overview of the known transcriptional regulation of gluconeogenesis. To effectively switch to a glycolytic state after glucose re-entry, cells rapidly down-regulate the gluconeogenic machinery. The gluconeogenic enzymes Pck1 and Fbp1 are regulated by a GID complex-mediated ubiquitination and proteasomal degradation. However, the glucose-mediated regulation of the gluconeogenic transcription factors remains unknown. *B,* glucose availability regulates amounts of the gluconeogenic activator Rds2. Cells were grown in glucose-replete or glucose-deplete (glycerol/ethanol) medium, and Rds2 protein amounts were compared by Western blotting using anti-FLAG antibody (see under "Experimental procedures"). Coomassie-stained gel showing total protein was used as the loading control. A representative blot (from three independent experiments) is shown. *C,* glucose addition results in a rapid reduction in Rds2 protein. Glucose was added to a final concentration of 3% to cells grown in glucose-deplete medium. Cells were collected at different time points post-glucose addition, and Rds2 amounts at each time were measured by Western blotting using anti-FLAG antibody. Cells grown in glucose-deplete medium (glycerol/ethanol), without the addition of glucose, were used as a control. Loading control: Coomassie-stained gels showing total protein. Note: samples from the glucose addition experiment (*left panel*) and the control (no glucose addition, *right panel*) were resolved on separate gels. Relative Rds2 amounts from the representative gel for no glucose addition (*right panel*) are shown *below* the respective bands and were normalized relative to the *1st lane*. *D,* quantification of the blot in *C*, *left panel*, showing decrease in Rds2 upon glucose addition. The relative Rds2 amounts were quantified with respect to the Rds2 amount in cells collected at 0 min in glucose-deplete medium, using ImageJ, for three independent experiments. Data are displayed as means ± S.D., $n = 3$. *, $p < 0.05$.

cells, at 20 and 30 min post-glucose addition (Fig. 2*C*). This strongly suggested that glucose addition results in the proteasomal degradation of Rds2. We next asked whether Rds2 is conditionally ubiquitinated in response to glucose. For this, we added glucose to cells in the presence of MG132, immunopurified Rds2 ~20 min post-glucose addition, and probed for polyubiquitin conjugates (by Western blotting). We observed ubiquitin conjugates only in Rds2 immunoprecipitates from glucose-treated cells but not in the control cells where glucose was not added (Fig. 2*D*). These data suggest that Rds2 is specifically ubiquitinated rapidly in cells, in a glucose-dependent manner. Collectively, these data indicate that Rds2 is ubiquitinated and proteasomally degraded when glucose becomes available in the medium.

E3 ubiquitin ligase Pib1 interacts with and ubiquitinates Rds2

Ubiquitination is a multistep process mediated by the coordinated action of three enzymes: E1 (ubiquitin-activating), E2 (ubiquitin-conjugating), and E3 (ubiquitin ligase). Ubiquitination substrate specificity depends on the E3 ubiquitin ligase, which selectively binds to and ubiquitinates the target protein (32). Therefore, we hypothesized that in the presence of glucose an unidentified E3 ubiquitin ligase should specifically ubiquitinate Rds2 and regulate its degradation (Fig. 3*A*). We used

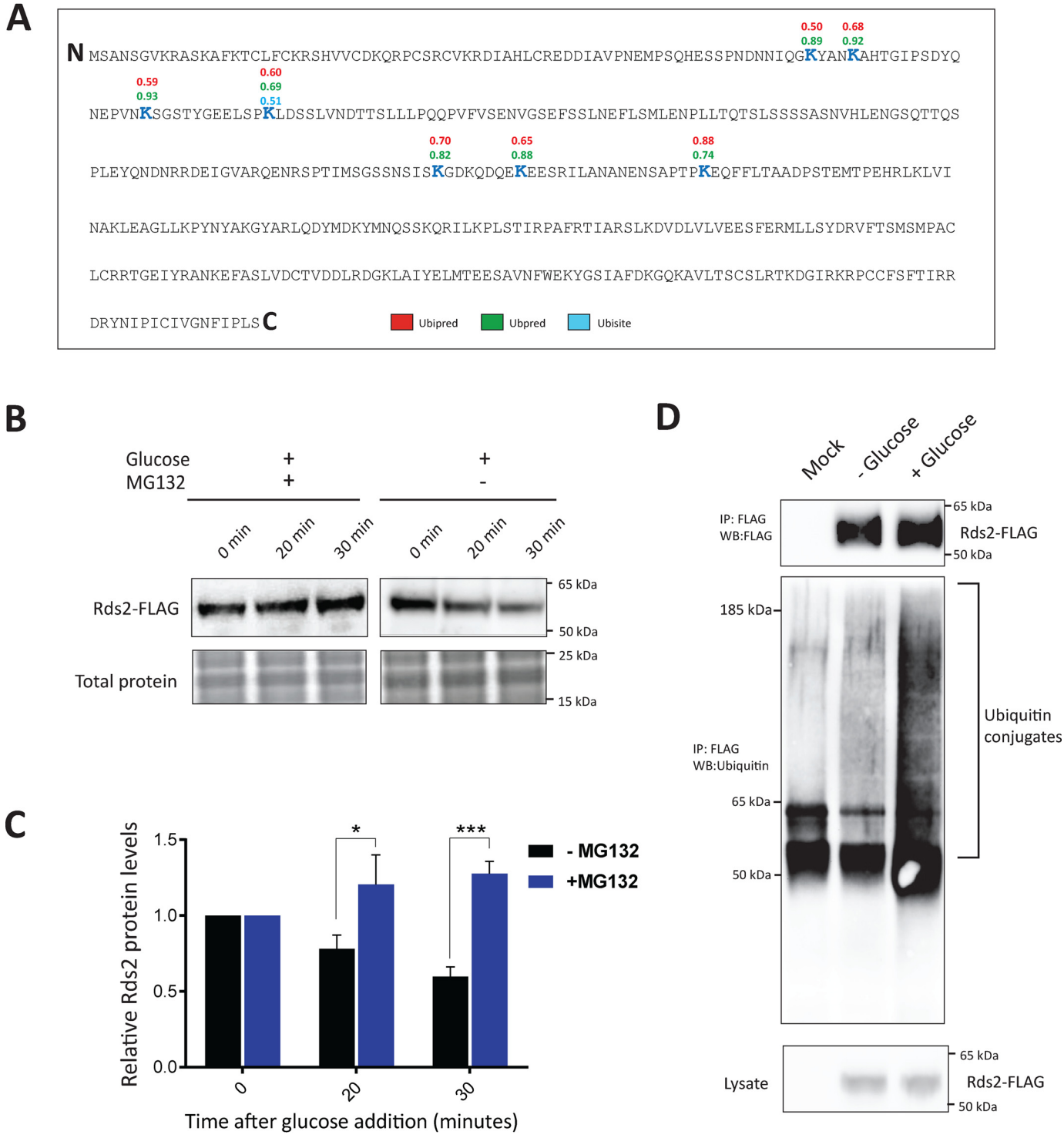

Figure 2. Glucose induces ubiquitination and proteasomal degradation of Rds2. *A,* putative ubiquitination sites in Rds2. We used three different ubiquitination prediction tools for identifying putative ubiquitin-binding lysine residues in Rds2. The high score lysine residues (scores greater than 0.5) recognized by at least two of the three analysis software are shown in the *schematic*. Individual scores of all the lysine residues from the predictions are shown in Fig. S1. *B,* glucose-dependent degradation of Rds2 is mediated by the proteasome. Cells expressing Rds2–FLAG grown in glucose-deplete medium were treated with glucose and MG132, and Rds2 amounts were measured by Western blotting. Note: these cells also lack the multidrug transporter Pdr5 to allow the MG132 accumulation in cells. Cells grown in glucose-deplete medium with the addition of glucose without MG132 addition were used as the control. Coomassie-stained gels were used as loading control. *C,* quantification of the blot in *B* using ImageJ. Data are displayed as means ± S.D., $n = 3$. *, $p < 0.05$; ***, $p < 0.001$. *D,* glucose addition induces ubiquitination of Rds2. Cells expressing Rds2–FLAG were grown in glucose-deplete medium and at an A_{600} ~0.8, and glucose was added at a final concentration of 3%. MG132 was also added along with glucose to prevent the degradation of ubiquitinated Rds2. Rds2–FLAG was immunoprecipitated after 20 min of glucose addition. Rds2–FLAG that was immunoprecipitated from cells grown in glucose-deplete medium without glucose addition but with MG132 treatment was used as control. Rds2– ubiquitin conjugates were detected by Western blotting using anti-ubiquitin antibody. A representative blot from at least three independent experiments is shown.

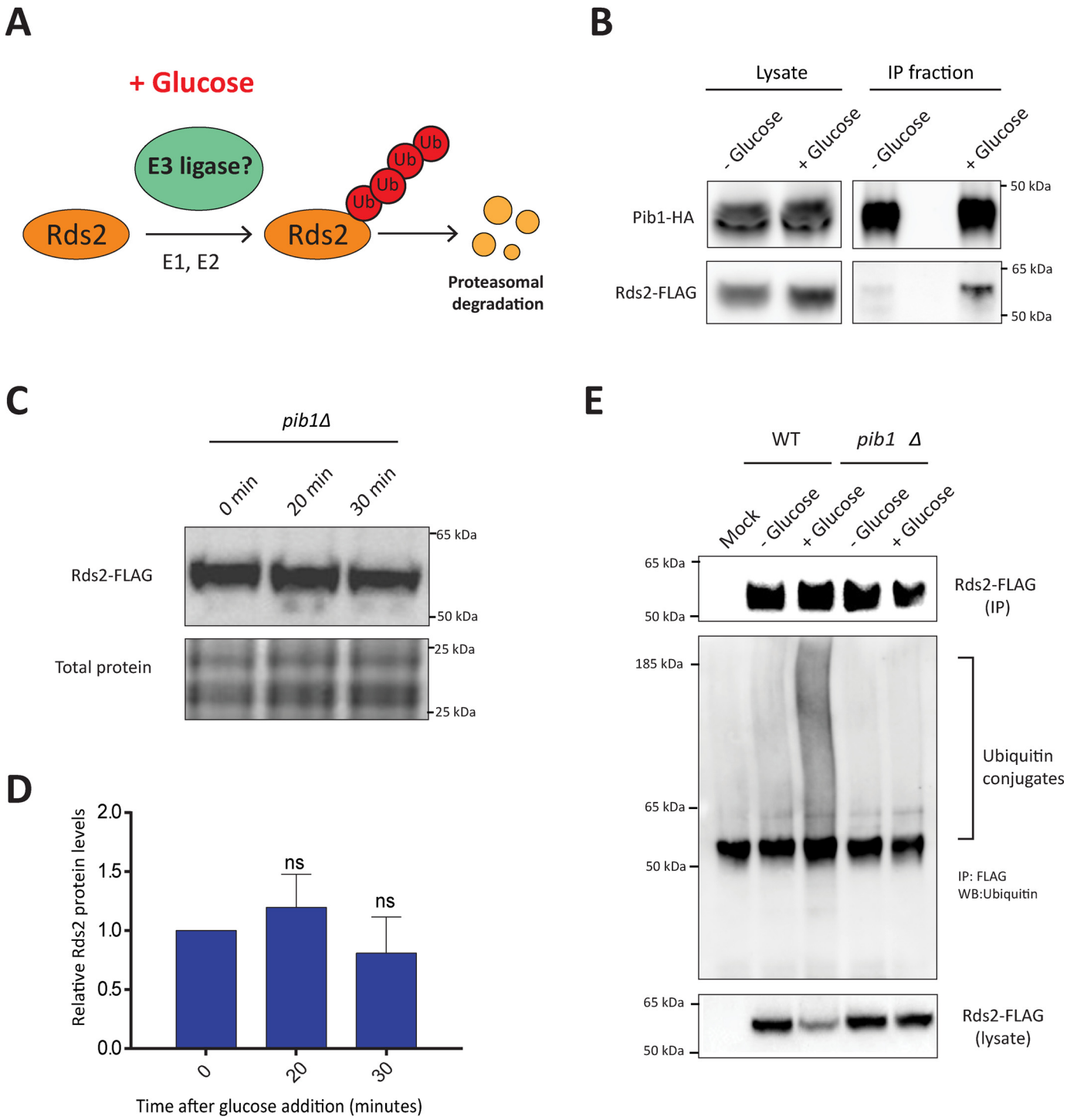

Figure 3. E3 ubiquitin ligase Pib1 interacts with and ubiquitinates Rds2. *A,* schematic illustrating a possible mechanism for glucose-mediated ubiquitination of Rds2, through an as-yet unknown E3 ubiquitin ligase. *B,* E3 ubiquitin ligase Pib1 interacts with Rds2 in a glucose-dependent manner. Pib1–HA was immunoprecipitated (*IP*) from glucose-treated (final concentration of 3%, 20-min treatment) and nontreated cells using an anti-HA antibody. The immunoprecipitated fractions were tested for the presence of Rds2–FLAG, using an anti-FLAG antibody, by Western blotting (*WB*). Also see File S1. *C,* Pib1 regulates glucose-mediated Rds2 degradation. Rds2–FLAG:*pib1*Δ cells grown in glucose-deplete medium were treated with glucose, and Rds2 protein was measured at different time points by Western blotting. *D,* quantification of the blot in *C* using ImageJ. Data are displayed as means ± S.D., $n = 3$. *n.s.*, not significant. *E,* Pib1 regulates glucose-mediated Rds2 ubiquitination. Rds2–FLAG was immunoprecipitated from glucose-treated (final concentration of 3%; 20-min treatment) and nontreated cells. Note: MG132 was added to all the samples to prevent degradation of ubiquitinated Rds2. The immunoprecipitated samples were separated on a 4–12% bis-tris gel, and Rds2– ubiquitin conjugates were detected by Western blotting using an anti-ubiquitin antibody.

YeastMine (46) to identify known interacting proteins of Rds2. This revealed Pib1, a protein with known E3 ligase activity, as an interacting protein partner of Rds2 (from other high-throughput studies (47)). Notably, this was the only putative Rds2-interacting protein with ubiquitin-related activity, as seen in the full list of physical interactors of Rds2 shown in File S1. This putative interaction of Rds2 with Pib1 and any possible function has remained unexplored. Therefore, to directly probe this

putative interaction, we performed co-immunoprecipitation studies by immunopurifying Pib1 (endogenously tagged at the C terminus with an HA epitope tag), and we tested whether Rds2 was associated with immunopurified Pib1. Notably, we performed these experiments using cells grown under two conditions: glucose-deplete medium (glycerol and ethanol as a carbon source); without the addition of glucose; or 20 min after glucose addition. Strikingly, we observed a strong co-immunopurification of Rds2 with Pib1, exclusively when Pib1 was isolated from cells minutes after glucose addition to the medium (Fig. 3*B*). As a control, we note that Pib1 amounts remain high and relatively constant regardless of the presence or absence of glucose (Fig. S2*A*). This strongly suggested that Pib1 interacts with Rds2 specifically when glucose became available (Fig. 3*B*).

Therefore, these data suggest a possible involvement of Pib1 in regulating glucose-mediated Rds2 ubiquitination. To address this possibility, we first monitored Rds2 amounts after glucose addition, in cells lacking Pib1 (*pib1*Δ). Notably, Rds2 amounts remained stable and did not decrease, even after ~30 min of glucose addition (Fig. 3, *C* and *D*). This was similar to the effect observed in cells treated with the proteasomal inhibitor MG132. Next, to determine whether Pib1 regulates Rds2 ubiquitination, we monitored the accumulation of polyubiquitin in Rds2 immunoprecipitates in *pib1*Δ cells. Strikingly, no Rds2–polyubiquitin conjugates were observed even in the presence of glucose in *pib1*Δ cells (Fig. 3*E*), in contrast to earlier observations made in WT cells. These data collectively show that Pib1 is required for the glucose-dependent ubiquitination and subsequent proteasomal degradation of Rds2 (Fig. 3*E*).

Pib1 ubiquitinates Rds2 in vitro

To determine whether Pib1 can directly act as the E3 ligase that ubiquitinates Rds2, we reconstituted an *in vitro* ubiquitination assay system. This assay requires incubating the substrate protein (Rds2), ATP, and ubiquitin with purified E1, E2, and E3 enzymes in a suitable reaction buffer, followed by Western blotting with anti-ubiquitin antibody to detect ubiquitin conjugates of the substrate (Fig. 4*A*). *S. cerevisiae* has a single E1 ubiquitin-activating enzyme Uba1 (48). We also utilized the E2 ubiquitin-conjugating enzyme Ubc4, because it has been used as an E2 ligase with Pib1 in a prior study (49). We first expressed recombinant Uba1 and Ubc4 (with C-terminal GST[2] tags) in *Escherichia coli*, and we subsequently purified these proteins (Fig. 4*B*). The GST tags were cleaved by TEV protease treatment and removed, and these purified E1 and E2 proteins were then utilized in predetermined amounts in the *in vitro* assay. Separately, we immunoprecipitated Rds2 (the substrate) and Pib1 (the E3-ligase) from cells treated with glucose (3% final concentration, 30 min treatment) to obtain sufficient amounts of the substrate and the E3 ligase. Note: Rds2 was immunopurified from *pib1*Δ cells to minimize Rds2 ubiquitination after glucose addition and to ensure that during immunoprecipitation neither Pib1 nor ubiquitin was eluted along with Rds2. BSA was used as a control protein in the reaction to test the substrate specificity of Pib1. Using this assay, with permutations of individual combinations of reagents (as indicated in Fig. 4*C*), robust Rds2– ubiquitin conjugates were observed exclusively when the E1, E2, Pib1, and ubiquitin (along with ATP) were present in the reaction mixture (Fig. 4*C*). Pib1 did not ubiquitinate the control protein in these conditions, and the E1 and E2 enzymes alone could not ubiquitinate Rds2 (Fig. 4*C*). These data show that Pib1 specifically and directly ubiquitinates Rds2 *in vitro*. Finally, to understand the glucose specificity of this process, we performed this *in vitro* ubiquitination assay using Rds2 (substrate) immunopurified from cells growing in glucose-deplete conditions, with or without glucose addition for ~30 min. Notably, small Rds2– ubiquitin conjugates were observed with Rds2 immunoprecipitated from cells without glucose addition, whereas strong polyubiquitination was observed in Rds2 immunopurified from cells post-glucose addition (Fig. 4*D*). This confirms that Pib1-mediated Rds2 ubiquitination is glucose-dependent. Collectively, these data establish Pib1 as the E3 ubiquitin ligase that ubiquitinates Rds2 upon glucose re-availability, leading to Rds2 degradation.

Pib1 preferentially ubiquitinates dephosphorylated Rds2

Our results shows that Pib1-mediated ubiquitinations of Rds2 are specific to the presence of glucose. However, how Pib1 specifically ubiquitinates Rds2 only in the presence of glucose remains unclear. One possibility is that glucose-mediated post-translational modification(s) on Rds2 regulate the ability of Pib1 being able to ubiquitinate Rds2. Interestingly, in our earlier Western blottings we noted a difference in mobility of Rds2 protein in glucose-deplete medium compared with glucose-replete medium (Fig. 1, *B* and *C*). Reduced electrophilic mobility of proteins is often indicative of post-translational modifications, notably phosphorylation, and earlier studies have suggested Rds2 phosphorylation (39). To rigorously confirm whether there is a glucose-dependent differential migration of Rds2 in SDS-polyacrylamide gels, cells expressing Rds2–FLAG were grown in glucose-deplete medium, and glucose was added at a final concentration of 3%. These cells were collected at different time intervals after glucose addition; proteins were extracted and resolved on a gradient gel (4–12% bis-tris), and Rds2 was detected by Western blotting. We observed that Rds2 from cells collected at 20 and 60 min post-glucose addition migrated faster compared with that of the 0-min time point (Fig. 5*A*), confirming a glucose-dependent differential mobility of Rds2. To determine whether this is because of the phosphorylation status of Rds2, we immunopurified Rds2–FLAG from cells grown in glucose-deplete medium before and 60 min after glucose addition. Furthermore, the immunopurified sample from glucose-deplete cells were treated with Antarctic phosphatase. These samples were resolved on a 7% SDS-PAGE, and Rds2–FLAG was detected by Western blotting. We observed that Rds2 from cells grown in glucose-deplete medium showed two bands in the blot (Fig. 5*B*). After phosphatase treatment, the lower band was the predominant band suggesting that the higher band observed in the blot was due to the phosphorylated state of Rds2. Furthermore, Rds2 immunopurified 60 min after glucose treatment was predominantly present as the lower

[2] The abbreviations used are: GST, glutathione *S*-transferase; bis-tris, 2-[bis(2-hydroxyethyl)amino]-2-(hydroxymethyl)propane-1,3-diol; TEV, tobacco etch virus; PEP, phosphoenolpyruvate; 3PG, 3-phosphoglycerate; qRT, quantitative RT; PTM, post-translational modification.

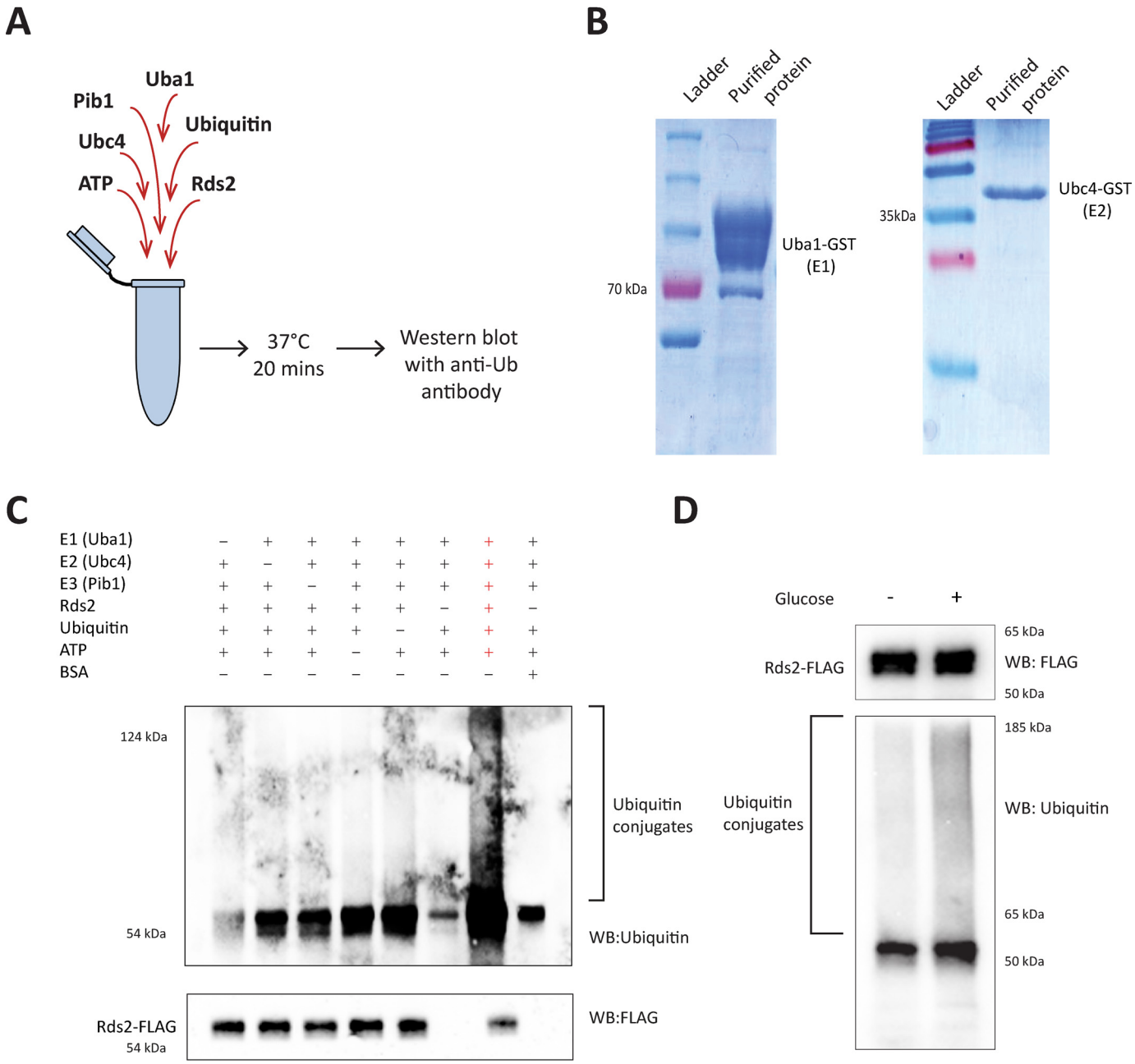

Figure 4. Pib1 ubiquitinates Rds2 *in vitro*. *A,* schematic illustration of the *in vitro* ubiquitination assay design, to test for the ability of Pib1 to specifically ubiquitinate Rds2 *in vitro*. *B,* purification of recombinant E1 and E2 enzymes. GST-tagged E1 (Uba1) and E2 (Ubc4) enzymes were recombinantly expressed in BL21 (DE3) cells and purified by GSH-affinity chromatography. The purified fractions run on SDS-PAGE and stained with Coomassie Blue are shown. *C,* Pib1p ubiquitinates Rds2 *in vitro*. An *in vitro* ubiquitination assay was set up with the following components in the reaction mixture: *E1* (Uba1p); *E2* (Ubc4p); *E3* (Pib1p-FLAG); the substrate (Rds2–FLAG or BSA-BSA as a control), ubiquitin, $MgCl_2$, and ATP. Note: GST tags of Uba1 and Ubc4 were removed using TEV protease treatment prior to their use in the *in vitro* assay to avoid any interference from the tags. Rds2–FLAG and Pib1–FLAG were immunoprecipitated from cells grown in glucose-deplete medium and treated with glucose (final concentration of 3%) for 30 min. Rds2–FLAG was immunoprecipitated from *pib1*Δ cells to prevent its ubiquitination, to minimize the presence of ubiquitin bound Rds2 in the immunoprecipitation fraction. The mixture was incubated for 20 min at 37 °C, and the reaction was terminated by adding SDS-PAGE sample buffer. The mixture was run on a 10% SDS-PAGE gel, and Western blotting (*WB*) was done using anti-FLAG (to detect Rds2–FLAG and Pib1–FLAG) or anti-ubiquitin (to detect Rds2– ubiquitin conjugates) antibodies. *D,* Pib1-mediated Rds2 ubiquitination is specific to the presence of glucose. An *in vitro* ubiquitination assay was performed using Rds2 immunoprecipitated from glucose-deplete cells (in *pib1*Δ strain background), either before glucose addition or 30 min after glucose addition (final concentration of 3%), to determine whether ubiquitination of Rds2 by Pib1 was glucose-dependent. The samples were run on a 4–12% gel, and ubiquitin conjugates were detected by Western blotting with anti-ubiquitin antibody.

band (Fig. 5*B*). These data suggest that Rds2 is phosphorylated in glucose-deplete medium, and after the glucose addition, the major form of Rds2 is its dephosphorylated form. To determine whether this glucose-mediated differential phosphorylation of Rds2 affected ubiquitination, we performed an *in vitro* ubiquitination assay using Rds2 immunopurified from glucose-deplete cells, with or without phosphatase treatment, as well as 60 min after glucose addition. We observed that ubiquitination of Rds2 (immunopurified from glucose-deplete medium) is substantially higher in phosphatase-treated samples, compared with

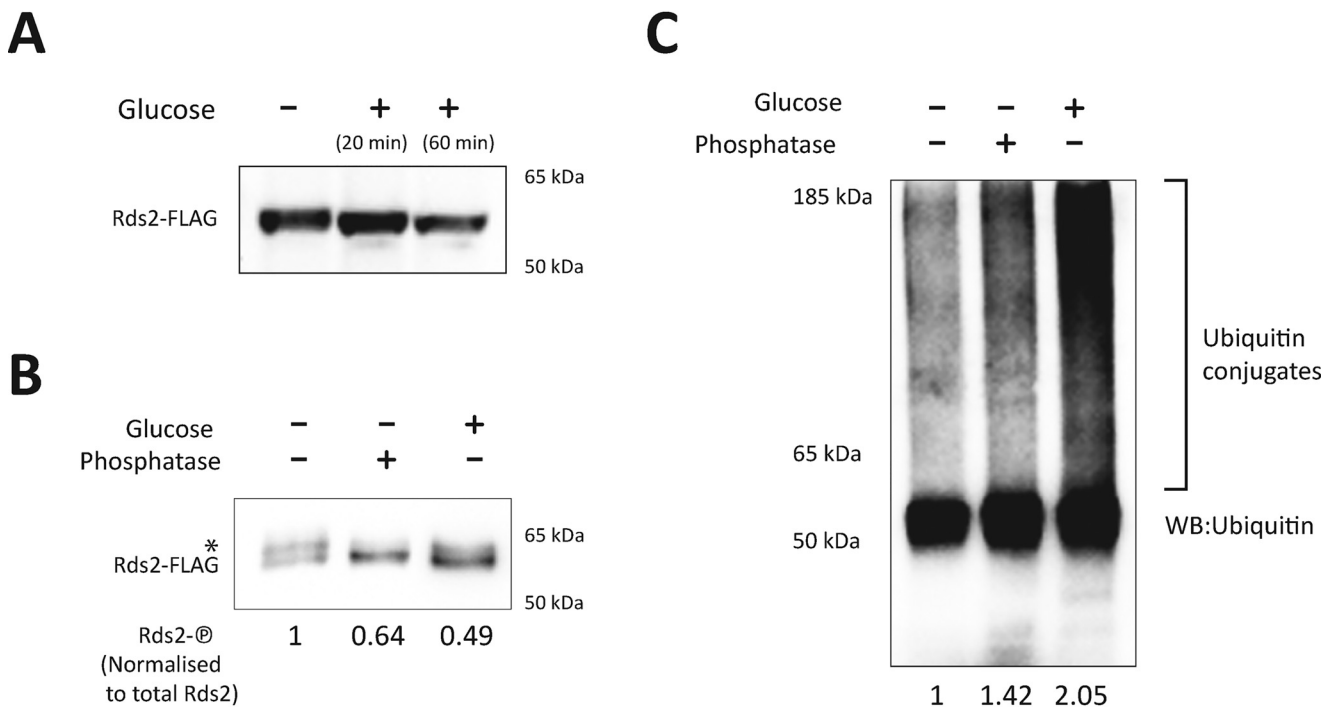

Figure 5. Pib1 preferentially ubiquitinates the dephosphorylated form of Rds2. *A,* electrophoretic mobility of Pib1 in glucose-deplete or -replete conditions. Cells expressing Rds2–FLAG were grown in glucose-deplete medium at an A_{600} ~0.8, and glucose was added to a final concentration of 3%. Samples were collected at the 0-, 20-, and 60-min time points post-glucose addition. Rds2 protein bands at different time points were detected using Western blotting. *B*, Rds2 is phosphorylated in glucose-deplete medium. Rds2–FLAG was immunopurified from cells grown in glucose-deplete with or without glucose treatment (3% final glucose concentration, 60 min treatment). The Rds2–FLAG immunoprecipitated from glucose-deplete medium– grown cells were treated with Antarctic Phosphatase (from New England Biolabs) and incubated at 37 °C for 1 h. The samples were run on a 7% SDS gel, and Rds2 was detected by Western blotting (*WB*) using anti-FLAG antibody. Quantification of Rds2 phosphorylation was done using ImageJ. The relative phosphorylation band intensities (normalized to total Rds2) are shown. *Asterisk* denotes the phosphorylated protein. *C,* dephosphorylated Rds2 is preferentially ubiquitinated. Rds2–FLAG was immunopurified from cells grown in glucose-deplete medium with or without glucose treatment (3% final glucose concentration, 30 min treatment). The concentrations of the immunoprecipitated protein samples were determined using BCA protein estimation method. The protein sample from cells grown in glucose-deplete medium was treated with Antarctic Phosphatase (from New England Biolabs). An *in vitro* ubiquitination assay was set up for these samples, and Rds2– ubiquitin conjugates were detected by Western blotting using anti-ubiquitin antibody. Quantification of the blot was done using ImageJ.

samples without phosphatase treatment (Fig. 5*C*). Note: because the amounts of Rds2 in the immunopurified samples were normalized, and equal amounts of Rds2 were added to the *in vitro* assay reaction mixtures, any difference in the extent of Rds2 ubiquitination observed was due to differences in Rds2–ubiquitin-conjugate formation and not due to amounts of Rds2 in the reaction mixture. This suggests that the dephosphorylated form of Rds2 is more prone to ubiquitination compared with its phosphorylated form. Collectively, our data show that Rds2 exists in a dephosphorylated state in the presence of glucose and that the dephosphorylated form of Rds2 promotes its glucose-mediated ubiquitination.

Pib1 is required for normal gluconeogenic flux and glucose repression after glucose addition

Because Rds2 transcriptionally activates the gluconeogenic enzyme genes, *FBP1* and *PCK1*, and also inhibits the GID complex that regulates the degradation of Pck1 and Fbp1 proteins in response to glucose (39), we therefore tested whether cells lacking Pib1 have higher levels of Fbp1 and Pck1 proteins compared with WT cells. For this, we estimated the protein levels of Pck1 and Fbp1 in WT and *pib1*Δ cells grown in glucose-deplete medium, before and after glucose addition. Glucose was added to a final concentration of 3%, and cells were collected 30 min post-glucose addition. Consistently, we observed significantly higher levels of Pck1 in *pib1*Δ cells compared with WT cells. Interestingly, the steady-state Pck1 protein levels were significantly higher in *pib1*Δ cells compared with WT cells, even in glucose-deplete medium (Fig. 6*A*). In *pib1*Δ cells, in the presence of glucose, Pck1 protein levels remained similar to that of glucose-deplete medium and were significantly higher compared with the Pck1 levels in WT cells post-glucose addition (Fig. 6*A*). We did not observe any difference in Fbp1 protein levels in *pib1*Δ cells compared with that of WT cells (Fig. 6*A*). We further estimated the transcript levels of these genes in WT and *pib1*Δ cells at different time points after glucose addition by qRT-PCR. We observed significantly higher mRNA levels of both *FBP1* and *PCK1* in *pib1*Δ cells ~1-h post-glucose addition, compared with the WT cells (Fig. S3*A*). These data all strongly suggest a role of Pib1 in regulating key gluconeogenic enzymes at the level of transcription (both Pck1 and Fbp1) and translation (Pck1).

These data collectively suggest that Pib1 must regulate normal gluconeogenic flux. To directly determine the role of Pib1 in regulating the rate of gluconeogenesis, we devised a stable isotope-based quantitative and targeted metabolic flux analysis (by LC-MS/MS) to measure gluconeogenic flux before and after glucose addition in WT and *pib1*Δ cells. Aspartate can be used as a carbon source for gluconeogenesis after being converted to

oxaloacetate (Fig. 6*B*), and hence by using a pulse of stable carbon isotope-labeled aspartate ([$^{13}C_4$]aspartate), gluconeogenic flux can be measured by estimating the ^{13}C label incorporation in gluconeogenic intermediates. We first estimated gluconeogenic flux in WT and *pib1*Δ cells in glucose-deplete medium. Cells were grown in glucose-deplete (glycerol/ethanol)

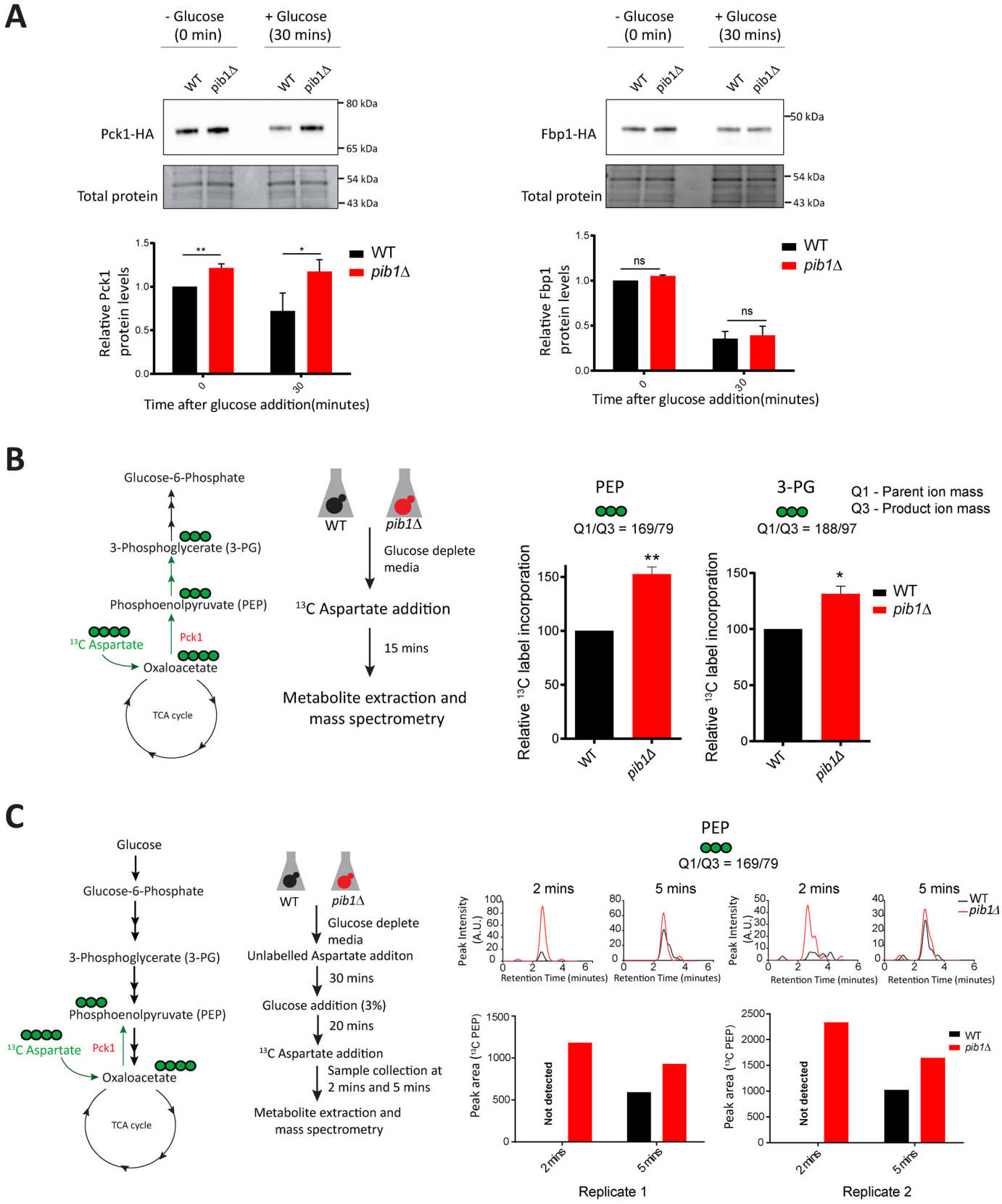

medium, shifted to minimal medium without amino acid supplementation, and [$^{13}C_4$]aspartate was added as illustrated in Fig. 6*B*. The [$^{13}C_4$]aspartate pulse was added 2 h post-shift to minimal medium, and 15 min later metabolites were extracted, and label incorporation into gluconeogenic intermediates was measured by LC-MS/MS (Fig. 6*B*). We observed a significantly higher label incorporation in the early gluconeogenic intermediates PEP and 3-PG in *pib1*Δ cells compared with WT cells (Fig. 6*B*). This functionally corroborates our earlier observation that steady-state protein levels of Pck1 are higher in *pib1*Δ cells compared with that of WT cells. These data suggest that loss of Pib1 results in an imbalanced gluconeogenic state, and the flux toward gluconeogenesis is higher than WT cells even in glucose-deplete medium. To determine whether Pib1 is required for efficient shutting down of gluconeogenesis post-glucose addition, we estimated flux into PEP from gluconeogenesis in WT and *pib1*Δ cells, after glucose addition to cells grown in glucose-deplete medium (*i.e.* in glycolytic conditions). Briefly, WT and *pib1*Δ cells were grown in glucose-deplete (glycerol/ethanol) medium, and shifted to minimal medium (with the same carbon sources), without amino acid supplementation. Note: to confirm that shifting to minimal medium before glucose addition does not unusually alter Rds2 degradation, we estimated Rds2 protein levels 2 h post-shift to this minimal medium at different time points after glucose addition. We observed a decrease in Rds2 levels after glucose addition, similar to what was observed in our earlier experiments using complex (yeast extract/peptone) medium (Fig. S3*B*). We also ensured that the cells are adapted to utilizing aspartate by adding 1 mM unlabeled aspartate to cells 1.5 h after the shift to minimal medium. At 2 h post-shifting to minimal medium, glucose was added at a final concentration of 3%. After 20 min post-glucose addition, the cells were pulse-labeled with 1 mM [$^{13}C_4$]aspartate and metabolites extracted at 2 and 5 min post-[$^{13}C_4$]aspartate addition, and label incorporation into gluconeogenic intermediates was measured (Fig. 6*C*). We observed higher levels of PEP in *pib1*Δ cells compared with WT cells in samples collected at 2 min as well as 5 min post-[$^{13}C_4$]aspartate addition (Fig. 6*C*). Notably, PEP could not be reliably detected in WT cells in ~2 min, in stark contrast to *pib1*Δ cells (where it was easily detected) (Fig. 6). Furthermore, PEP was substantially lower in WT cells (compared with *pib1*Δ cells) after 5 min. These data show that the loss of Pib1 results in an inefficient shut down of gluconeogenesis after glucose addition. Collectively, these data show that Pib1 regulates the effective shutdown of gluconeogenesis and glucose repression upon glucose re-entry into the medium.

Pib1 regulates competitive cell-growth fitness post-glucose addition

Finally, we tested the functional implications of inefficient gluconeogenic shutdown (after glucose addition), using a competitive growth fitness assay with WT and *pib1*Δ cells. WT and *pib1*Δ cells (identified using different drug selection markers) were grown separately in glucose-replete, or glucose-deplete medium, and equal numbers of these cells (based on absorbance at 600 nm) were mixed together in either glucose-replete or glucose-deplete medium. Cells were plated on drug selection plates at different time intervals, and the relative numbers of WT and *pib1*Δ cells were calculated by colony counting. This experimental design is illustrated in Fig. 7*A*. Under conditions when cells are transferred from glucose-poor to glucose-replete medium, the *pib1*Δ cells should not be able to efficiently switch to glycolysis (*i.e.* show efficient glucose repression) compared with WT cells. This would therefore predict that WT cells will outcompete *pib1*Δ cells in growth. Indeed, we observed that the relative number of WT cells is significantly higher compared with *pib1*Δ cells after the switch to a glucose-replete medium, for around 4.5 h (Fig. 7*A*), consistent with the observation that *pib1*Δ cells sustain gluconeogenesis upon glucose reentry. Eventually, over longer times, the *pib1*Δ cells eventually catch up with the WT cells. Notably, in control experiments (where the cells were grown and mixed in glucose-replete medium), both WT and *pib1*Δ cells showed equal numbers of cells (Fig. 7*A*). Also interestingly, when cells were grown and mixed together in glucose-deplete (glycerol/ethanol) medium, *pib1*Δ cells outcompeted WT cells around 6 h after the shift (Fig. 7*A*), and this is also consistent with a functional role for Pib1 in regulating a gluconeogenic state. This also correlates with our earlier observations that the gluconeogenic flux is higher in *pib1*Δ cells compared with WT cells when grown in glucose-deplete medium (Fig. 6*B*). Collectively, these data suggest that Pib1 regulates the ability of cells to efficiently switch to a glucose-repressed state by controlling the amounts of the gluconeogenic regulator Rds2 upon glucose re-entry.

Figure 6. Pib1 regulates gluconeogenic flux and shutdown post-glucose addition. *A,* Pck1 protein levels are higher in *pib1*Δ cells compared with WT cells. WT and *pib1*Δ cells expressing Pck1–HA and Fbp1–HA were grown in glucose-deplete medium, and glucose was added to a final concentration of 3%. Cells were collected at 0 and 30 min post-glucose addition. Pck1–HA and Fbp1–HA were detected by Western blotting (using an anti-HA antibody). The quantification of the blot was done using ImageJ. Data are displayed as means ± S.D., $n = 3$. *, $p < 0.05$; **, $p < 0.01$; significance is based on a Student's *t* test (using GraphPad Prism 7.0). *n.s.*, not significant. Total protein concentration estimates and Coomassie-stained gels were used as loading control. *B,* flux toward PEP and 3PG synthesis is higher in *pib1*Δ cells. Aspartate is converted into oxaloacetate and enters gluconeogenesis as a carbon source, as shown in the *schematic*. Gluconeogenic flux can be measured by pulse-labeling with a stable isotope ($^{13}C_4$) of aspartate and measuring the carbon-label incorporation into gluconeogenic intermediates. WT and *pib1*Δ cells were grown in glucose-deplete medium, shifted to a minimal medium (same carbon source) without amino acid supplementation, and 2 h post-shift, the cells were pulse-labeled with [$^{13}C_4$]aspartate for 15 min. The cells were quenched, and the gluconeogenic intermediates PEP and 3PG were measured by LC-MS/MS. The relative ^{13}C label incorporation is shown. Data are displayed as means ± S.D., $n = 3$. *, $p < 0.05$; **, $p < 0.01$. Significance is based on a Student's *t* test (using GraphPad Prism 7.0). *C,* Pib1 is required for efficient shutdown of gluconeogenesis after glucose addition. WT and *pib1*Δ cells were grown in glucose-deplete medium, shifted to a minimal medium without amino acid supplementation, and 2 h post-shift, glucose was added to a final concentration of 3%. The cells were pulse-labeled with [$^{13}C_4$]aspartate 20 min post-glucose addition. The cells were collected at 2 and 5 min after [$^{13}C_4$]aspartate pulse and quenched, and the gluconeogenic intermediates PEP and 3PG were measured by LC-MS/MS. The ^{13}C label incorporation in PEP and 3PG are plotted, along with (*insets*) the actual MS/MS spectra for the two cell types. Data are displayed as means ± S.D., $n = 3$. *, $p < 0.05$; **, $p < 0.01$; significance is based on a Student's *t* test (using GraphPad Prism 7.0).

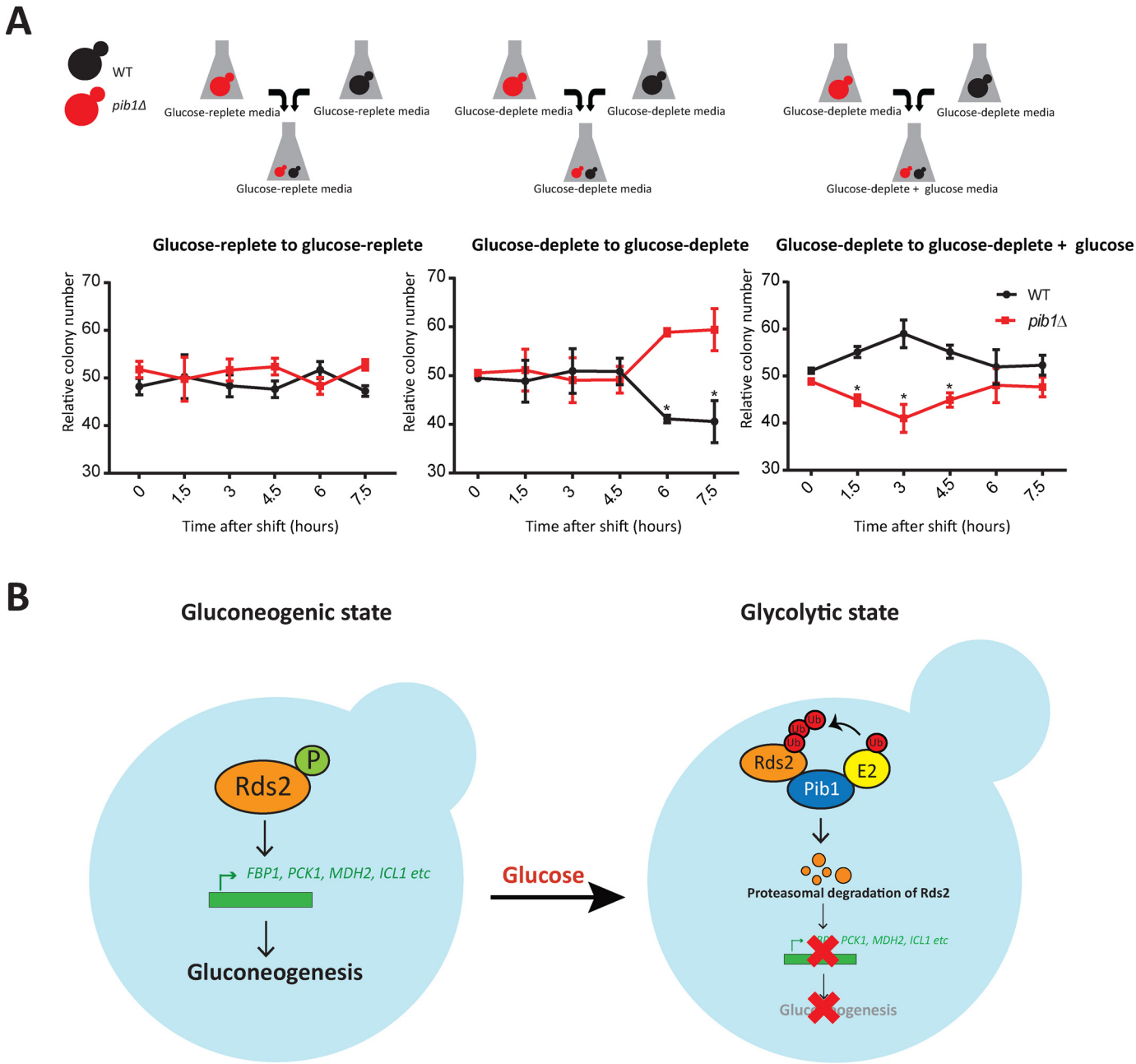

Figure 7. Pib1 regulates the competitive cell-growth fitness post-glycolytic switch. *A, pib1*Δ cells show a growth fitness defect in competitive growth assays upon glucose addition. WT and *pib1*Δ cells were cultured in either glucose-replete or glucose-deplete medium, and equal amounts of cells were mixed together and transferred to glucose-replete medium, glucose-deplete medium (2% glycerol/ethanol), or glucose-deplete medium supplemented with glucose (final concentration of 3%), with a starting cell density based on A_{600} of 0.2 each. This experimental design is illustrated. Subsequently, cells were collected and plated on appropriate selection plates, to quantify relative amounts of each genetic background. The relative genetic background is shown. Data are displayed as means ± S.D., $n = 3$. *, $p < 0.05$, significance is based on a Student's *t* test. *B,* proposed model illustrating the role of Pib1 in regulating glucose-mediated Rds2 degradation. In glucose-deplete cells, Rds2 in its active, phosphorylated form transcriptionally activates the expression of different gluconeogenic and glyoxylate cycle enzymes, enforcing a gluconeogenic state. Upon glucose addition, Rds2 is dephosphorylated. Pib1 interacts with and ubiquitinates Rds2, and targets it for proteasomal degradation. This ensures proper gluconeogenic shutdown and complete glucose repression.

Discussion

In this study, we identify a functional role for the E3 ubiquitin ligase Pib1 as a regulator of gluconeogenesis and a mediator of effective gluconeogenic shutdown upon glucose re-entry into the medium. Pib1 binds to and mediates the glucose-dependent ubiquitination and subsequent proteasomal degradation of the gluconeogenic transcription factor Rds2. Pib1-mediated ubiquitination of Rds2 depends on the phosphorylation state of Rds2. Finally, quantitative gluconeogenic flux measurements, as well as competitive growth experiments, suggest a role for Pib1 in mediating effective glucose repression. Collectively, our data suggest a role for Pib1 as an "off-switch" for gluconeogenesis and as a mediator of effective glucose repression.

We first characterized glucose-mediated Rds2 regulation, and by using this as our readout, our aim was to identify regulators involved in down-regulating the gluconeogenic tran-

scription factors, when glucose becomes available to cells. Upon glucose entry, Rds2 protein amounts rapidly decrease over time (Fig. 1). This glucose-mediated decrease in Rds2 amounts is due to its ubiquitin-mediated proteasomal degradation (Fig. 2). Although similar responses have been previously identified with respect to the regulation of gluconeogenic and glyoxylate cycle enzymes themselves, our study shows how a key transcription factor that controls gluconeogenic enzyme transcripts is regulated in the presence of glucose and uses this as a way to identify novel regulators of the overall transcriptional state of the cell with changing nutrients (in this case glucose re-entry).

Through this, we identify a glucose-dependent, ubiquitin-mediated signaling response, with the E3 ubiquitin ligase Pib1 as a mediator of this response. Strikingly, the interaction of Pib1 with Rds2 is very specific to the re-availability of glucose (Fig. 3). Furthermore, the loss of *PIB1* prevents Rds2 ubiquitination and its proteasomal degradation even in the presence of glucose (Fig. 3). This interaction of Pib1 with Rds2 and its role in ubiquitinating Rds2 is direct and glucose-dependent (Fig. 4). Furthermore, Rds2 is present predominantly in a dephosphorylated form after glucose addition, and this dephosphorylated form is more prone to ubiquitination by Pib1 (Fig. 5). Finally, we find that functionally Pib1 regulates the amounts of gluconeogenic enzyme Pck1 and controls overall gluconeogenic flux (Fig. 6). Thereby Pib1 regulates cell growth and competitive fitness post-glucose addition (Fig. 7). Collectively, these observations reveal a novel, functional role for Pib1 as a regulator of the glucose-mediated ubiquitination and proteasomal degradation of Rds2 and effective glucose repression in yeast. Although previous studies have suggested the role of Pib1 in regulating vacuolar sorting (50), and a recent study has identified the exocyst subunit Sec3p as a Pib1-specific target in *Schizosaccharomyces pombe* (51), no function of Pib1 in regulating responses to nutrients is currently known. These results add a dimension to recent studies that suggest roles of E3 ubiquitin ligases as regulators of metabolic states (36, 52). The glucose-dependent, Pib1-mediated regulation of a gluconeogenesis master regulator occurs minutes after glucose addition, reiterating the swiftness of the response. Because E3 ligases can ubiquitinate specific sets of substrates, an exciting future area of investigation will be to identify all substrates of Pib1 in a glucose-dependent context.

The ubiquitination machinery is itself regulated at multiple levels, and apart from E3 ligases that conjugate ubiquitin to specific targets, the deubiquitination machinery removes ubiquitins from target proteins (53, 54). This involves deubiquitinase enzymes that bind to specific ubiquitinated proteins and cleave the bound ubiquitins, to coordinately achieve a tight, reversible regulation of protein ubiquitination. The role of deubiquitinase enzymes in metabolic state switching has largely remained entirely unexplored. Our experimental approach, to observe early ubiquitination responses to the re-entry of nutrients, might reveal additional such regulators. Finally, the cross-talk of ubiquitination with other post-translational modifications, notably acetylation and phosphorylation (55, 56), is a poorly-explored but interesting mode of signaling regulation. How this cross-talk between PTMs activates or inhibits target protein ubiquitination, in the context of different nutrient cues, is poorly explored. Our results reveal an intriguing cross-talk of the Pib1 ubiquitin machinery with phosphorylation, in mediating Rds2 regulation. This hints at the possibility of a glucose-responsive phosphatase that dephosphorylates Rds2 following glucose re-entry, thereby favoring its ubiquitination by Pib1. If this is true, identifying this phosphatase could reveal more details about general signaling events regulating glucose repression. Emerging studies suggest that acetylation and phosphorylation can regulate the ubiquitination and degradation of metabolic enzymes in other model systems as well (57). The combinatorial effect of these PTMs could therefore result in a sensitive, tightly-controlled, and rapidly responsive metabolic switching machinery. Thus, the complex network of metabolic state regulation machinery involving E3 ubiquitin ligases, deubiquitinases, kinases, phosphatases, acetylases, and deacetylases opens an interesting arena of post-translational modification-mediated regulation of metabolic switching.

Experimental procedures

Yeast strains, media, and growth conditions

The prototrophic CEN.PK strain (WT) was used in all experiments (58). All the strains used in this study are listed in Table S1. The gene deletion and C-terminal chromosomal tagging were done using the standard PCR-based gene deletion and modification strategy (59). The media used in this study were glucose-deplete media (1% yeast extract, 2% peptone, 2% ethanol, and 1% glycerol) and glucose-replete media (1% yeast extract, 2% peptone, and 2% dextrose). For experiments involving the addition of glucose to cells grown in glucose-deplete media, cells were initially grown at 30 °C to an A_{600} of 0.8, and glucose was added to a final concentration of 3%. All experiments involving MG132 were done in a *pdr5*Δ background to prevent the efflux of MG132 by the multidrug transporter protein Pdr5. A final concentration of 100 μM MG132 was used in all the experiments involving proteasomal inhibition.

Protein extraction and Western blotting

When the cells reach an A_{600} of 0.8, 10 ml of the culture cells were collected and pelleted, and protein extraction was performed using the trichloroacetic acid (TCA) extraction method. Briefly, the pelleted cells were resuspended in 400 μl of 10% TCA solution, and the cells were lysed by bead beating (three times, 20 s each with 1 min of cooling in ice-water slurry between each cycle). Lysate extracts were centrifuged, and the protein pellets thus obtained were resuspended in 400 μl of SDS/glycerol buffer (7.3% SDS, 29.1% glycerol, and 83.3 mM Tris base) and heated for 10 min at 100 °C. The supernatant was collected after centrifugation (20,000 × *g*/10 min), and total protein estimation was done using BCA assay (BCA assay kit, G-Biosciences). Samples were normalized (to maintain constant protein amounts) in SDS/glycerol buffer. The samples were run on 4–12% bis-tris gels (Invitrogen) unless specified otherwise. Western blots were developed using the following antibodies: anti-FLAG M2 (mouse mAb, Sigma); anti-HA (12CA5 mouse mAb, Roche Applied Science); anti-ubiquitin (P4D1 mouse mAb, CST); and anti-FLAG (D6W5B rabbit mAb, CST). Horseradish peroxidase-conjugated secondary

antibodies (mouse and rabbit) were obtained from CST. For developing the blot, standard enhanced chemiluminescence reagent (WesternBright ECL HRP substrate, Advansta) was used. Coomassie-stained gels were used as the loading controls. The quantification of the blots was done using ImageJ. The statistical significance was determined using Student's *t* test (using GraphPad Prism 7.0)

Immunoprecipitation and co-immunoprecipitation

Cells were grown in glucose-deplete media with or without glucose addition as specified and 50 A_{600} of cells were harvested by centrifugation. The collected cells were lysed in lysis buffer (50 mM HEPES buffer, pH 7.5, 50 mM sodium fluoride, 10% glycerol, 150 mM KCl, 1 mM EDTA, 2 mM sodium orthovanadate, 2 mM phenylmethylsulfonyl fluoride, 0.1 mM leupeptin, 0.02 mM pepstatin, 0.25% Tween 20) using a mini bead beater. The lysate was incubated with Dynabeads Protein G (Invitrogen) and conjugated with the required antibody for 3 h at 4 °C. The lysate was collected, and the beads were washed five times in wash buffer (50 mM HEPES buffer, pH 7.5, 50 mM sodium fluoride, 10% glycerol, 150 mM KCl, 1 mM EDTA, 2 mM sodium orthovanadate, 0.05% Tween 20). The bound proteins were eluted by boiling the samples in SDS-PAGE sample buffer (for HA-tagged proteins) or by FLAG peptide elution (for FLAG-tagged proteins, using 0.5 mg/ml FLAG peptide). The samples were then subjected to Western blotting. For co-immunoprecipitation studies with Pib1 and Rds2, HA-tagged Pib1 was immunoprecipitated using the above-described method and eluted by boiling in SDS-PAGE sample buffer. Rds2–FLAG was detected in the elution fraction by Western blotting using anti-FLAG antibody.

In vivo ubiquitination assay

Rds2–FLAG was immunoprecipitated from glucose-treated and nontreated cultures using anti-FLAG M2 antibody (mouse mAb, Sigma) and eluted by FLAG peptide elution. The eluted proteins were run on a 10% polyacrylamide gel and subjected to Western blotting. The presence of Rds2–FLAG in the lysate and elution fractions was detected using anti-FLAG antibody (D6W5B rabbit mAb, CST). To detect Rds2– ubiquitin conjugates, anti-ubiquitin antibody (P4D1 mouse mAb, CST) was used.

In vitro ubiquitination assay

Uba1–GST and Ubc4–GST were expressed in *E. coli* BL21(DE3) cells using pGST parallel plasmids and purified using GSH-affinity chromatography. Briefly, the lysate was passed through a column containing GSH resin. The bound proteins were eluted using an elution buffer containing 10 mM reduced GSH. The GST tags were removed using His_6-tagged TEV protease treatment, followed by passing it through a column containing GSH resin. The TEV protease was removed by passing this sample through a nickel-nitrilotriacetic acid column. The concentrations of the purified proteins were estimated using Bradford estimation method. Rds2–FLAG was immunoprecipitated from *pib1*Δ cells grown in glucose-deplete medium (with or without glucose treatment) and Pib1–FLAG from *rds2*Δ cells grown in glucose-deplete medium, treated with glucose (final concentration of 3%, 30 min treatment) and eluted by FLAG peptide elution. The concentrations of these proteins were estimated by BCA protein estimation method (BCA assay kit, G-Biosciences). The *in vitro* ubiquitination assay was set up with the following components in the reaction mixture: 100 nM Uba1, 1 μM Ubc4, 1 μM Pib1-FLAG, 5 μM Rds2-FLAG, 100 μM ubiquitin, 1X ubiquitination buffer (50 mM Tris-HCl, pH-8, 5 mM $MgCl_2$, 0.1 % Tween 20, 1 mM DTT), 2 mM ATP. The mixture was incubated for 20 min at 37 °C, and the reaction was terminated by adding SDS-PAGE sample buffer. The samples were run on a 10% polyacrylamide gel, and ubiquitin chains were detected by Western blotting with anti-ubiquitin antibody (P4D1 mouse mAb, CST).

Phosphatase treatment of the immunoprecipitated samples

Rds2–FLAG immunoprecipitated from glucose-deplete medium was treated with Antarctic phosphatase (from New England Biolabs) as per the manufacturer's protocol. 1 unit of the enzyme was used per μg of the protein sample, and the reaction mixture was incubated at 37 °C for 1 h. The reaction was stopped by adding 4× SDS-PAGE sample buffer to the reaction followed by boiling the samples at 95 °C for 5 min.

Metabolite extraction and LC-MS/MS analysis

To measure the difference in gluconeogenic flux in WT and *pib1*Δ cells, we performed a stable isotope labeling–based quantitative metabolic flux analysis (60). Briefly, the cells were grown in glucose-deplete medium, and at an A_{600} ~0.8, they were shifted to synthetic minimal media without amino acid supplementation to minimize the interference from an unlabeled amino acid pool during labeled aspartate incorporation. At 2 h post-shift, 1 mM [$^{13}C_4$]aspartate (Cambridge Isotope laboratories) was pulsed. Metabolites were quenched and extracted 15 and 60 min post-[$^{13}C_4$]aspartate pulse, as explained in detail elsewhere (60). To measure the gluconeogenic flux post-glucose addition, cells were grown in glucose-deplete medium, and at an A_{600} ~0.8 they were shifted to synthetic minimal media without amino acid supplementation. Unlabeled aspartate (1 mM final concentration) was added to the cells 1.5 h post-shift, to allow cells to adapt to the presence of aspartate (as a carbon source for gluconeogenesis). At 2 h post-shift to minimal medium, glucose was added to the cells at a final concentration of 3%. 20 min post-glucose addition, [$^{13}C_4$]aspartate was pulsed, and metabolites were quenched and extracted 2 and 5 min post-[$^{13}C_4$]aspartate addition, following protocols described elsewhere (60). The dried extracts were resuspended in 50 μl of 25% acetonitrile in 5 mM ammonium acetate. We used Synergi^{TM} 4-μm Fusion-RP 80-Å (×100, 4.6 mm) LC column for detection, and the indicated metabolites were estimated using an ABSciex QTRAP 6500 in triple-quadrupole mode. The solutions used for separation were 5 mM ammonium acetate in water (solvent A) and acetonitrile (solvent B). Detailed flow-parameters are described in Ref. 60.

RNA isolation and RT-qPCR

RNA isolation was done using a hot acid phenol extraction method. Briefly, cells were grown in glucose-deplete media and five A_{600} cells were harvested by centrifugation. The pellets

were resuspended in 400 μl of TES solution (10 mM Tris-HCl, pH 7.5, 10 mM EDTA, and 0.5% SDS). To this, 400 μl of acid phenol was added and mixed by vortexing. The resuspended pellets were incubated at 65 °C for 60 min with intermittent vortexing. The supernatant was collected after centrifugation and subjected to another round of acid phenol treatment followed by incubation and intermittent vortexing as before. The supernatant obtained by centrifugation was treated with 400 μl of chloroform and mixed, and the aqueous phase obtained after centrifugation was collected. To this, 40 μl of 3 M sodium acetate, pH 5.3, and 1 ml of ice-cold 100% ethanol were added. This mixture was incubated at −20 °C for 60 min. RNA was pelleted by centrifugation and washed in ice-cold 70% ethanol. The pellet was air-dried and resuspended in nuclease-free water. The isolated RNA was quantified and treated with Turbo DNase (Invitrogen). DNase-treated RNA was then used for cDNA synthesis using Superscript III reverse transcriptase (Invitrogen) as per the manufacturer's protocol. The cDNA was then used to perform qRT-PCR using the KAPA SYBR FAST qRT-PCR master mix kit (KK4602, KAPA Biosystems) as per the manufacturer's instructions. Actin (*ACT1*) was used as a control to normalize the values obtained. The mRNA fold change was calculated by a standard 2[caret]−(ΔΔ*Ct*) method. The statistical significance was determined using Student's *t* test (using GraphPad Prism 7.0).

Competitive growth fitness assay

WT and *pib1*Δ cells carrying different drug selection markers were cultured separately in either glucose-replete or glucose-deplete medium. At an A_{600} ~0.8, they were subcultured together at a starting A_{600} of 0.2 each, in either glucose-replete medium, glucose-deplete medium, or glucose-deplete medium supplemented with glucose (final concentration of 3%). Samples were collected from this mixed culture at 0, 1.5, 3, 4.5, 6, and 7.5 h and were serially diluted to a final concentration of ~3000 cells per ml. 100 μl of this was plated on appropriate drug selection plates in triplicate and incubated at 30 °C. The number of colonies was counted, and the relative percentage of WT and *pib1*Δ colonies at each time point was calculated. These values obtained were plotted, and the statistical significance was determined using Student's *t* test (using GraphPad Prism 7.0).

Author contributions—V. V. and S. L. conceptualization; V. V. and Z. R. data curation; V. V., Z. R., and S. L. formal analysis; V. V. validation; V. V., Z. R., and S. L. investigation; V. V. and S. L. visualization; V. V., Z. R., and S. L. methodology; V. V. and S. L. writing-original draft; S. L. supervision; S. L. funding acquisition; S. L. project administration; S. L. writing-review and editing.

Acknowledgments—We acknowledge the extensive use of the inStem/NCBS/CCAMP MS facilities in this study. We acknowledge Swagata Adhikary for helping with the protein purification and in vitro ubiquitination experiments.

References

1. Broach, J. R. (2012) Nutritional control of growth and development in yeast. *Genetics* **192,** 73–105 CrossRef Medline
2. Dechant, R., and Peter, M. (2008) Nutrient signals driving cell growth. *Curr. Opin. Cell Biol.* **20,** 678–687 CrossRef Medline
3. Efeyan, A., Comb, W. C., and Sabatini, D. M. (2015) Nutrient-sensing mechanisms and pathways. *Nature* **517,** 302–310 CrossRef Medline
4. Zaman, S., Lippman, S. I., Zhao, X., and Broach, J. R. (2008) How *Saccharomyces* responds to nutrients. *Annu. Rev. Genet.* **42,** 27–81 CrossRef Medline
5. Ljungdahl, P. O., and Daignan-Fornier, B. (2012) Regulation of amino acid, nucleotide, and phosphate metabolism in *Saccharomyces cerevisiae*. *Genetics.* **190,** 885–929 CrossRef Medline
6. Ochocki, J. D., and Simon, M. C. (2013) Nutrient-sensing pathways and metabolic regulation in stem cells. *J. Cell Biol.* **203,** 23–33 CrossRef Medline
7. Yuan, H. X., Xiong, Y., and Guan, K. L. (2013) Nutrient sensing, metabolism, and cell growth control. *Mol. Cell* **49,** 379–387 CrossRef Medline
8. Lindsley, J. E., and Rutter, J. (2004) Nutrient sensing and metabolic decisions. *Comp. Biochem. Physiol. B Biochem. Mol. Biol.* **139,** 543–559 CrossRef Medline
9. De Deken, R. H. (1966) The Crabtree effect: a regulatory system in yeast. *J. Gen. Microbiol.* **44,** 149–156 CrossRef Medline
10. Diaz-Ruiz, R., Rigoulet, M., and Devin, A. (2011) The Warburg and Crabtree effects: On the origin of cancer cell energy metabolism and of yeast glucose repression. *Biochim. Biophys. Acta* **1807,** 568–576 CrossRef Medline
11. Postma, E., Verduyn, C., Scheffers, W. A., and Van Dijken, J. P. (1989) Enzymic analysis of the Crabtree effect in glucose-limited chemostat cultures of *Saccharomyces cerevisiae*. *Appl. Environ. Microbiol.* **55,** 468–477 Medline
12. Schüller, H.-J. (2003) Transcriptional control of nonfermentative metabolism in the yeast *Saccharomyces cerevisiae*. *Curr. Genet.* **43,** 139–160 CrossRef Medline
13. Wang, Y., Pierce, M., Schneper, L., Güldal, C. G., Zhang, X., Tavazoie, S., and Broach, J. R. (2004) Ras and Gpa2 mediate one branch of a redundant glucose signaling pathway in yeast. *PLos Biol.* **2,** E128 CrossRef Medline
14. Zaman, S., Lippman, S. I., Schneper, L., Slonim, N., and Broach, J. R. (2009) Glucose regulates transcription in yeast through a network of signaling pathways. *Mol. Syst. Biol.* **5,** 245 CrossRef Medline
15. Fiechter, A., and Seghezzi, W. (1992) Regulation of glucose metabolism in growing yeast cells. *J. Biotechnol.* **27,** 27–45 CrossRef
16. Holzer, H. (1976) Catabolite inactivation in yeast. *Trends Biochem. Sci.* **1,** 178–181 CrossRef
17. van de Poll, K. W., 2[caret]−(ΔΔ*Ct*) method, A., and Schamhart, D. H. (1974) Isolation of a regulatory mutant of fructose 1,6-diphosphatase in *Saccharomyces carlsbergensis*. *J. Bacteriol.* **117,** 965–970 Medline
18. Carlson, M. (1999) Glucose repression in yeast. *Curr. Opin. Microbiol.* **2,** 202–207 CrossRef Medline
19. van den Brink, J., Canelas, A. B., van Gulik, W. M., Pronk, J. T., Heijnen, J. J., de Winde, J. H., and Daran-Lapujade, P. (2008) Dynamics of glycolytic regulation during adaptation of *Saccharomyces cerevisiae* to fermentative metabolism. *Appl. Environ. Microbiol.* **74,** 5710–5723 CrossRef Medline
20. Kresnowati, M. T., van Winden, W. A., Almering, M. J., ten Pierick, A., Ras, C., Knijnenburg, T. A., Daran-Lapujade, P., Pronk, J. T., Heijnen, J. J., and Daran, J. M. (2006) When transcriptome meets metabolome: fast cellular responses of yeast to sudden relief of glucose limitation. *Mol. Syst. Biol.* **2,** 49 CrossRef Medline
21. Hackett, S. R., Zanotelli, V. R., Xu, W., Goya, J., Park, J. O., Perlman, D. H., Gibney, P. A., Botstein, D., Storey, J. D., and Rabinowitz, J. D. (2016) Systems-level analysis of mechanisms regulating yeast metabolic flux. *Science* **354,** aaf2786–15 CrossRef Medline
22. Yin, Z., Hatton, L., and Brown, A. J. (2000) Differential post-transcriptional regulation of yeast mRNAs in response to high and low glucose concentrations. *Mol. Microbiol.* **35,** 553–565 CrossRef Medline
23. Tripodi, F., Nicastro, R., Reghellin, V., and Coccetti, P. (2015) Post-translational modifications on yeast carbon metabolism: regulatory mechanisms beyond transcriptional control. *Biochim. Biophys. Acta* **1850,** 620–627 CrossRef Medline

24. Rolland, F., Winderickx, J., and Thevelein, J. M. (2002) Glucose-sensing and -signalling mechanisms in yeast. *FEMS Yeast Res.* **2,** 183–201 CrossRef Medline
25. Xiong, Y., McCormack, M., Li, L., Hall, Q., Xiang, C., and Sheen, J. (2013) Glucose-TOR signalling reprograms the transcriptome and activates meristems. *Nature* **496,** 181–186 CrossRef Medline
26. Kim, J. H., Roy, A., Jouandot, D., 2nd., and Cho, K. H. (2013) The glucose signaling network in yeast. *Biochim. Biophys. Acta* **1830,** 5204–5210 CrossRef Medline
27. Wilson, W. A., and Roach, P. J. (2002) Nutrient-regulated protein kinases in budding yeast. *Cell* **111,** 155–158 CrossRef Medline
28. Cantó, C., and Auwerx, J. (2010) AMP-activated protein kinase and its downstream transcriptional pathways. *Cell. Mol. Life Sci.* **67,** 3407–3423 CrossRef Medline
29. Bononi, A., Agnoletto, C., De Marchi, E., Marchi, S., Patergnani, S., Bonora, M., Giorgi, C., Missiroli, S., Poletti, F., Rimessi, A., and Pinton, P. (2011) Protein kinases and phosphatases in the control of cell fate. *Enzyme Res.* **2011,** 329098 CrossRef Medline
30. Komander, D., and Rape, M. (2012) The ubiquitin code. *Annu. Rev. Biochem.* **81,** 203–229 CrossRef Medline
31. Glickman, M. H., and Ciechanover, A. (2002) The ubiquitin-proteasome proteolytic pathway: destruction for the sake of construction. *Physiol. Rev.* **82,** 373–428 CrossRef Medline
32. David, Y., Ternette, N., Edelmann, M. J., Ziv, T., Gayer, B., Sertchook, R., Dadon, Y., Kessler, B. M., and Navon, A. (2011) E3 ligases determine ubiquitination site and conjugate type by enforcing specificity on E2 enzymes. *J. Biol. Chem.* **286,** 44104–44115 CrossRef Medline
33. Hershko, A., and Ciechanover, A. (1998) The ubiquitin system. *Annu. Rev. Biochem.* **67,** 425–479 CrossRef Medline
34. Benanti, J. A., Cheung, S. K., Brady, M. C., and Toczyski, D. P. (2007) A proteomic screen reveals SCFGrr1 targets that regulate the glycolytic-gluconeogenic switch. *Nat. Cell Biol.* **9,** 1184–1191 CrossRef Medline
35. Nakatsukasa, K., Nishimura, T., Byrne, S. D., Okamoto, M., Takahashi-Nakaguchi, A., Chibana, H., Okumura, F., and Kamura, T. (2015) The ubiquitin ligase SCF^{Ucc1} acts as a metabolic switch for the glyoxylate cycle. *Mol. Cell* **59,** 22–34 CrossRef Medline
36. Santt, O., Pfirrmann, T., Braun, B., Juretschke, J., Kimmig, P., Scheel, H., Hofmann, K., Thumm, M., and Wolf, D. H. (2008) The yeast GID complex, a novel ubiquitin ligase (E3) involved in the regulation of carbohydrate metabolism. *Mol. Biol. Cell* **19,** 3323–3333 CrossRef Medline
37. Schork, S. M., Thumm, M., and Wolf, D. H. (1995) Catabolite inactivation of fructose-1,6-bisphosphatase of *Saccharomyces cerevisiae*. *J. Biol. Chem.* **270,** 26446–26450 CrossRef Medline
38. Jin, X., Pan, Y., Wang, L., Zhang, L., Ravichandran, R., Potts, P. R., Jiang, J., Wu, H., and Huang, H. (2017) MAGE–TRIM28 complex promotes the Warburg effect and hepatocellular carcinoma progression by targeting FBP1 for degradation. *Oncogenesis* **6,** e312 CrossRef Medline
39. Soontorngun, N., Larochelle, M., Drouin, S., Robert, F., and Turcotte, B. (2007) Regulation of gluconeogenesis in *Saccharomyces cerevisiae* is mediated by activator and repressor functions of Rds2. *Mol. Cell. Biol.* **27,** 7895–7905 CrossRef Medline
40. Hedges, D., Proft, M., and Entian, K. D. (1995) CAT8, a new zinc cluster-encoding gene necessary for derepression of gluconeogenic enzymes in the yeast *Saccharomyces cerevisiae*. *Mol. Cell. Biol.* **15,** 1915–1922 CrossRef Medline
41. Vincent, O., and Carlson, M. (1998) Activator, binds to the carbon source-responsive element of gluconeogenic genes. *EMBO J.* **17,** 7002–7008 CrossRef Medline
42. Schüle, T., Rose, M., Entian, K. D., Thumm, M., and Wolf, D. H. (2000) Ubc8p functions in catabolite degradation of fructose-1,6-bisphosphatase in yeast. *EMBO J.* **19,** 2161–2167 CrossRef Medline
43. Wang, W., and Subramani, S. (2017) Role of PEX5 ubiquitination in maintaining peroxisome dynamics and homeostasis. *Cell Cycle* **16,** 2037–2045 CrossRef Medline
44. Radivojac, P., Vacic, V., Haynes, C., Cocklin, R. R., Mohan, A., Heyen, J. W., Goebl, M. G., and Iakoucheva, L. M. (2010) Identification, analysis and prediction of protein ubiquitination sites. *Proteins* **78,** 365–380 CrossRef Medline
45. Tung, C. W., and Ho, S. Y. (2008) Computational identification of ubiquitylation sites from protein sequences. *BMC Bioinformatics* **9,** 310 CrossRef Medline
46. Balakrishnan, R., Park, J., Karra, K., Hitz, B. C., Binkley, G., Hong, E. L., Sullivan, J., Micklem, G., and Cherry, J. M. (2012) YeastMine–an integrated data warehouse for *Saccharomyces cerevisiae* data as a multipurpose tool-kit. *Database* **2012,** bar062 CrossRef Medline
47. Uetz, P., Giot, L., Cagney, G., Mansfield, T. A., Judson, R. S., Knight, J. R., Lockshon, D., Narayan, V., Srinivasan, M., Pochart, P., Qureshi-Emili, A., Li, Y., Godwin, B., Conover, D., Kalbfleisch, T., *et al.* (2000) A comprehensive analysis of protein ± protein interactions in *Saccharomyces cerevisiae*. *Nature* **403,** 623–627 CrossRef Medline
48. McGrath, J. P., Jentsch, S., and Varshavsky, A. (1991) UBA 1: an essential yeast gene encoding ubiquitin-activating enzyme. *EMBO J.* **10,** 227–236 CrossRef Medline
49. Shin, M. E., Ogburn, K. D., Varban, O. A., Gilbert, P. M., and Burd, C. G. (2001) FYVE domain targets Pib1p ubiquitin ligase to endosome and vacuolar membranes. *J. Biol. Chem.* **276,** 41388–41393 CrossRef Medline
50. MacDonald, C., Winistorfer, S., Pope, R. M., Wright, M. E., and Piper, R. C. (2017) Enzyme reversal to explore the function of yeast E3 ubiquitin-ligases. *Traffic* **18,** 465–484 CrossRef Medline
51. Kampmeyer, C., Karakostova, A., Schenstrøm, S. M., Abildgaard, A. B., Lauridsen, A. M., Jourdain, I., and Hartmann-Petersen, R. (2017) The exocyst subunit Sec3 is regulated by a protein quality control pathway. *J. Biol. Chem.* **292,** 15240–15253 CrossRef Medline
52. Nakatsukasa, K., Okumura, F., and Kamura, T. (2015) Proteolytic regulation of metabolic enzymes by E3 ubiquitin ligase complexes: lessons from yeast. *Crit. Rev. Biochem. Mol. Biol.* **50,** 489–502 CrossRef Medline
53. Pickart, C. M., and Rose, I. A. (1985) Ubiquitin carboxyl-terminal hydrolase acts on ubiquitin carboxyl-terminal amides. *J. Biol. Chem.* **260,** 7903–7910 Medline
54. Komander, D., Clague, M. J., and Urbé, S. (2009) Breaking the chains: structure and function of the deubiquitinases. *Nat. Rev. Mol. Cell Biol.* **10,** 550–563 CrossRef Medline
55. Hunter, T. (2007) The age of crosstalk: phosphorylation, ubiquitination, and beyond. *Mol. Cell* **28,** 730–738 CrossRef Medline
56. Caron, C., Boyault, C., and Khochbin, S. (2005) Regulatory cross-talk between lysine acetylation and ubiquitination: role in control of protein stability. *BioEssays* **27,** 408–415 CrossRef Medline
57. Jiang, W., Wang, S., Xiao, M., Lin, Y., Zhou, L., Lei, Q., Xiong, Y., Guan, K. L., and Zhao, S. (2011) Acetylation regulates gluconeogenesis by promoting PEPCK1 degradation via recruiting the UBR5 ubiquitin ligase. *Mol. Cell* **43,** 33–44 CrossRef Medline
58. van Dijken, J. P., Bauer, J., Brambilla, L., Duboc, P., Francois, J. M., Gancedo, C., Giuseppin, M. L., Heijnen, J. J., Hoare, M., Lange, H. C., Madden, E. A., Niederberger, P., Nielsen, J., Parrou, J. L., Petit, T., *et al.* (2000) An interlaboratory comparison of physiological and genetic properties of four *Saccharomyces cerevisiae* strains. *Enzyme Microb. Technol.* **26,** 706–714 CrossRef Medline
59. Longtine, M. S., McKenzie, A., 3rd., Demarini, D. J., Shah, N. G., Wach, A., Brachat, A., Philippsen, P., and Pringle, J. R. (1998) Additional modules for versatile and economical PCR-based gene deletion and modification in *Saccharomyces cerevisiae*. *Yeast* **14,** 953–961 CrossRef Medline
60. Walvekar, A., Rashida, Z., Maddali, H., and Laxman, S. (2018) A versatile LC-MS/MS approach for comprehensive, quantitative analysis of central metabolic pathways. *Wellcome Open Res.* **3,** 122 CrossRef Medline